Picosecond Structural Dynamics of Myoglobin following Photodissociation of Carbon Monoxide As Revealed by Ultraviolet Time-Resolved Resonance Raman Spectroscopy†

Akira Sato and Yasuhisa Mizutani*

Molecular Photoscience Research Center, Kobe University, 1-1 Rokkodai, Nada, Kobe 657-8501, Japan, and Core Research for Evolutional Science and Technology, Japan Science and Technology Agency, 4-1-8 Honmachi, Kawaguchi 332-0012, Japan

Received August 28, 2005; Revised Manuscript Received October 7, 2005

ABSTRACT: Picosecond protein dynamics of myoglobin in response to structural changes in heme upon CO dissociation were observed in a site-specific fashion for the first time using time-resolved UV resonance Raman spectroscopy. Transient UV resonance Raman spectra showed several phases of intensity changes in both tryptophan and tyrosine Raman bands. Five picoseconds after dissociation, the W18, W16, and W3 bands of tryptophan residues and the Y8a band of tyrosine residues decreased in intensity, followed by recovery of the Y8a band intensity in hundreds of picoseconds and recovery of the tryptophan bands in nanoseconds. These spectral changes suggest that the change in heme structure impulsively drives concerted movement of the EF helical section and that rearrangements toward a deoxy structure occur in the heme vicinity and in the A helix within a time frame of sub-nanoseconds to nanoseconds.

Protein dynamics are intimately connected to the structure−function relationship of biological systems. In numerous biological processes, protein structural changes resulting from reaction at a specific site must extend spatially to mesoscopic dimensions to elicit a biological function. The molecular mechanism of cooperativity in oxygen binding of hemoglobin (Hb)[1] is a classical example (*1*, *2*). The binding of small molecular ligands to the hemes in Hb is a highly localized perturbation. Nonetheless, this localized perturbation initiates a sequence of propagating structural events that culminates in a change in quaternary structure. The large-amplitude motions at the quaternary level, which form a communication link at the subunit interface, are driven by changes in the tertiary structure upon ligation. Thus, myoglobin (Mb), which is structurally very similar to a subunit of Hb, serves as a model system for tertiary relaxation processes.

The heme in Mb is an iron-protoporphyrin IX, in which the Fe^{2+} ion is bound to the proximal histidine (His) as the sole covalent link to the protein. The heme iron binds diatomic molecules, such as NO, CO, and O_2, at the opposite side of the proximal His. X-ray crystallography provided extensive information about the end point equilibrium structures (*3*). The magnitude of atomic displacement at the heme site required for ligand binding and release is estimated by examining the structures containing the heme with and without bound ligands. The ligated heme has a planar structure in which the low-spin iron atom is in the porphyrin plane. Upon ligand dissociation, the iron atom is converted from low- to high-spin and moves out of the porphyrin plane by approximately 0.3 Å. Structural changes in the heme associated with ligand dissociation result in conformational changes toward the deoxy structure.

Ultrafast optical absorption studies of Mb (*4*, *5*) revealed that the excited-state potential energy surface of the ligated heme is dissociative with regard to a ligand, to allow photoinitiation of a structural change from the ligated form to the deligated form within 50 fs with a quantum yield of nearly unity. These features of MbCO enabled us to optically trigger structural changes in a protein and to follow the accompanied structural relaxation using optical probes that are sensitive to aspects of the protein's motion. For these reasons, an enormous body of work has been generated concerning relaxation processes of Mb (*6*−*15*). Although the accumulated data suggest protein dynamics spanning subpicosecond to nanosecond time scales, most studies have examined structural changes in the heme group. Thus, details of structural changes in the protein moiety remain unclear.

Ultraviolet resonance Raman (UVRR) spectroscopy is a promising tool for studying protein structures because it permits observation of Raman bands of polypeptide backbones and aromatic amino acid residues with high selectivity (*16*−*18*). Several vibrational bands of aromatic residues function as structural markers of proteins; hence, time-resolved UVRR spectroscopy can provide site-specific information about protein dynamics. Despite successes in application of time-resolved UVRR spectroscopy to protein dynamics in the nanosecond to second region (*19*, *20*), application to protein dynamics in the picosecond region has

† This work was supported by a Grant-in-Aid for Specially Promoted Research (Grant 14001004) from the Ministry of Education, Culture, Sports, Science and Technology of Japan and a Grant-in-Aid for Scientific Research (B) (Grant 17350009) from the Japan Society for the Promotion of Science. This work also was partially supported by grants from the Kurata Memorial Hitachi Science and Technology Foundation, Shimadzu Science Foundation, and Hyogo Science and Technology Association.

* To whom correspondence should be addressed. E-mail: mizutani@kobe-u.ac.jp. Phone: +81-78-803-5705. Fax: +81-78-803-5705.

[1] Abbreviations: Hb, hemoglobin; Mb, myoglobin; UVRR, UV resonance Raman; BBO, β-barium borate; CCD, charge-coupled device.

10.1021/bi051732c CCC: $30.25
Published on Web 10/19/2005

only recently been reported (*21*). In this study, picosecond time-resolved UVRR spectroscopy was used to monitor structural changes in Mb following CO photodissociation, enabling site-specific observation of protein dynamics, including an impulsively driven protein response within a few picoseconds and subsequent structural rearrangements in sub-nanoseconds to nanoseconds.

MATERIALS AND METHODS

A Ti:sapphire oscillator-amplifier laser system provided pulses tuned to 800 nm with a repetition rate of 1 kHz. The second harmonic of the laser output was focused into a Raman shifter filled with 50 atm of methane gas to generate first Stokes stimulated scattering at 452 nm. A probe pulse at 226 nm was generated with a BBO crystal as the second harmonic of the 452 nm output. Components other than the 226 nm light were removed spatially with a Pellin-Broca prism and spectrally with dichroic mirrors which have high reflectivity in the range of 220−240 nm. Another portion of the 400 nm pulse passed through a variable delay stage was used as a pump pulse. After the pump and probe beams were made coaxial using a dichroic mirror, they were focused with spherical and cylindrical lenses onto the sample located in an airtight quartz NMR tube. Focused spot sizes were 150 μm × 5 mm for the probe beam and 200 μm × 5 mm for the pump beam. At the sample point, energies of the probe and pump pulses were 0.4 and 25 μJ, respectively. Temporal overlap was determined by difference frequency generation of visible pump and UV probe pulses in a thin BBO crystal. The cross correlation width between visible pump and UV probe pulses was measured to be 4.0 ps.

Raman scattered light was collected with an F/2 quartz doublet achromat and focused by an F/4 quartz doublet achromat onto the entrance slit of a prefilter (*22*) coupled to a single spectrograph (Spex, 500 M). The spectrograph was equipped with a 1200 grooves/mm, 500 nm blazed grating operating in second order, and dispersed light was detected with a liquid nitrogen-cooled CCD detector (Roper Scientific SPEC-10:400B/LN) with Unichrome UV-enhancing coating. Raman shifts were calibrated with cyclohexane to an accuracy of ±4 cm^{-1}. Data acquisition of picosecond time-resolved UVRR spectra was described previously (*23*).

Horse skeletal Mb (Sigma, M-0630) was dissolved in 50 mM sodium phosphate buffer at pH 7.7 to produce a 150 μM solution. For MbCO, the solution was placed in an airtight quartz NMR tube and reduced with sodium dithionite after five cycles of degassing and back-filling with CO. The sample solution was replaced with fresh solution every 60 min. The integrity of the sample after exposure to laser irradiation was confirmed by UV−vis absorption spectroscopy. The samples of deoxyMb were prepared by the same procedure used to prepare MbCO, except for back-filling with N_2 and equilibration of the sample under 1 atm of N_2. Just before the UVRR measurement, sodium perchlorate was added to the samples with a final concentration of 150 mM as an intensity standard.

RESULTS

Figure 1 shows the procedure for calculating picosecond UVRR difference spectra from unprocessed time-resolved spectra. Trace a is a probe-only spectrum, which represents

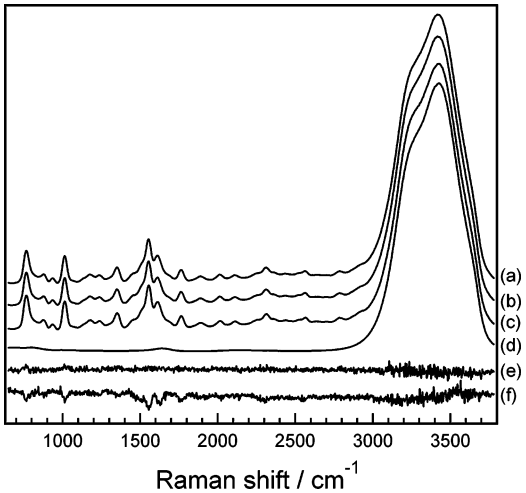

FIGURE 1: Procedure for calculation of picosecond UVRR spectra showing pump-induced differences. Nearly identical curves a−c are UVRR spectra corresponding to the (a) probe-only spectrum and pump−probe spectra with time delays of (b) −10 and (c) 5 ps. Curve d is the UVRR spectrum for the buffer solution. The contribution of quartz has been subtracted in traces a−d. Spectra a−c have been divided by a factor of 20. UVRR difference spectra e and f were generated by subtracting the probe-only spectrum from the pump−probe spectra at a delay of (b) −10 and (c) 5 ps, with an appropriate subtraction factor. The accumulation time at each time delay was 265 min.

the UVRR spectrum for MbCO. Traces b and c are pump−probe spectra with time delays of −10 and 5 ps, respectively. All distinct Raman bands in the spectra can be attributed to contributions from tryptophan (Trp) and tyrosine (Tyr) residues, except for a perchlorate band at 933 cm^{-1} and a strong water stretching band at 3300 cm^{-1}. In traces a−c, the quartz signal was removed from the spectra. The probe-only spectrum was subtracted from the pump−probe spectrum, providing the difference spectra shown in traces e (b − a) and f (c − a). For all of the difference spectra, the Raman bands of water and perchlorate were used as an internal standard. In trace e, no difference feature was observed for Trp and Tyr Raman bands at −10 ps; this corroborates the cross correlation measurement of 4.0 ps. In contrast, trace f shows the pump-induced negative difference features observed for the Trp and Tyr Raman bands, indicating deligation-induced intensity changes in the Raman bands. It should be noted that the water band was completely eliminated in traces e and f.

Figure 2 shows time-resolved UVRR difference spectra at delay times from −10 ps to 2.5 ns. The top trace represents the probe-only spectrum, while the bottom trace shows the deoxyMb minus MbCO difference spectrum. Raman bands of Trp and Tyr residues in the UVRR spectra were identified by comparison with UVRR spectra of aqueous amino acid solutions. Mode assignments made by Harada and co-workers were adopted (*17*). Following CO dissociation, the Trp and Tyr Raman bands showed stepwise intensity changes. The time evolution of integrated intensities of Trp and Tyr bands is shown in Figure 3. These changes are calculated relative to the respective intensities in the probe-only spectrum. At 5 ps, negative difference bands were observed at 763, 1012, 1553, and 1620 cm^{-1}, indicating that the photoproduct has weaker Raman bands than MbCO. The former three features can be ascribed to a decrease in intensity of the W18, W16, and W3 bands of Trp residues. The negative feature at 1620

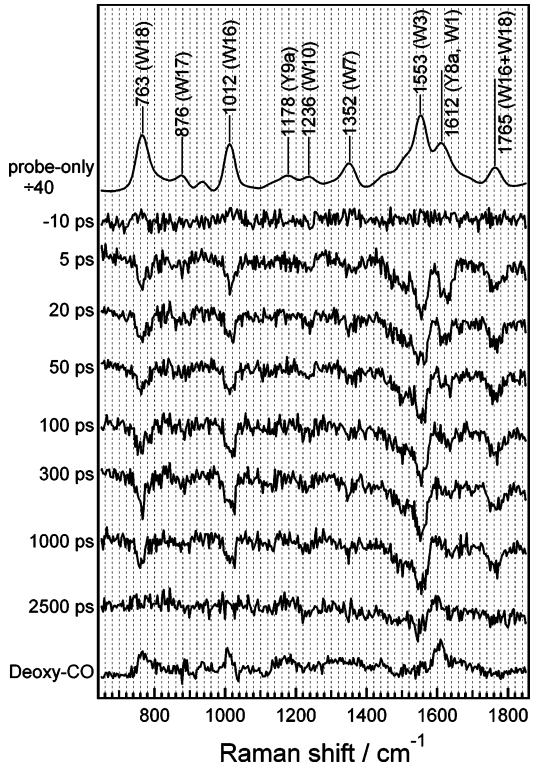

FIGURE 2: Picosecond UVRR difference spectra in the range of 650−1850 cm^{-1}. The probe-only spectrum, which represents the UVRR spectrum of MbCO, is divided by a factor of 40. The deoxyMb minus MbCO difference spectrum is depicted at the bottom for comparison. Spectra in the panel have been offset for clarity.

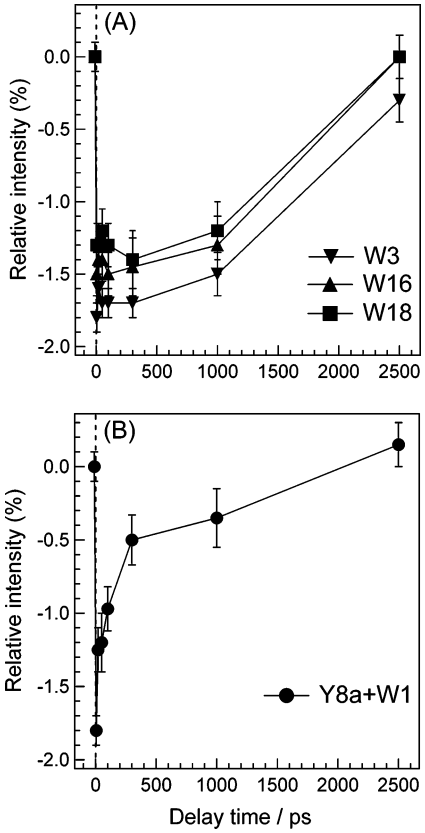

FIGURE 3: Intensity changes of UVRR bands relative to intensities in the probe-only spectrum as a function of delay time. Panels A and B display integrated intensities of Trp bands (W3, W16, and W18 modes) and that of sum of Y8a and W1 modes, respectively.

cm^{-1} is due to a reduction in intensity of the Y8a band of the Tyr residues, although an intensity change in the W1 band of the Trp residues also contributes. For delay times between 5 and 300 ps, the negative band at 1620 cm^{-1} decreased in intensity. In contrast, negative bands of the W18, W16, and W3 modes showed little change in intensity. The intensity of W1 with 226 nm excitation was less than one-third of that of the W3 band; the intensities of Trp bands other than that of W1 do not change, and therefore, the intensity decrease of the negative band at 1620 cm^{-1} can be attributed to recovery of the Y8a band intensity. The negative bands of the Trp residues, which exhibited little intensity change at 100 and 300 ps, decreased in intensity in the nanosecond region. While the negative bands of the W16 and W18 modes disappeared in the difference spectrum at a 2.5 ns time delay, the positive bands of these modes appeared in the equilibrium deoxyMb minus MbCO spectrum. This difference showed that structural rearrangements toward the deoxy structure are not completed within 2.5 ns.

DISCUSSION

In the application of UVRR spectroscopy to studies of protein structure, the intensity of Trp and Tyr Raman bands can be used as a probe of microenvironment near these residues, because changes in hydrogen bonding or local hydrophobicity will cause the shifts in the Raman excitation profiles (*24*, *25*). In the case presented here, the Raman intensity may change due to factors other than local structural changes in the protein. One possibility is that the photodissociated CO molecule diffusing within the protein can perturb the electronic state of aromatic residues. Time-resolved IR studies demonstrated that the photodissociated CO molecule is trapped in the docking site and remains at this site for 200 ns (*10*, *11*). The docking site is above the heme group (*6*) and far from the Trp and Tyr residues; hence, the CO molecule negligibly affects the Raman intensity of Tyr and Trp residues. Another possibility is a transient thermal effect on Raman scattering cross sections. Experimental studies on vibrational energy flow in Mb have shown that time constants of heme cooling and water heating are ~3 (*23*) and 7.5 ps (*26*), respectively. A time lag between heme cooling and water heating indicates that vibrational energy remains in the globin for several picoseconds. Thus, the local temperature of the Trp and Tyr residues transiently increases and may affect the intensity of Raman bands. Although observed intensity changes at 5 ps may be due to a transient thermal effect, this is not likely for the following reasons. The intensity of the Trp and Tyr bands at the 5 and 20 ps time delays showed no distinct difference, although most of the vibrational energy dissipates into the water at 20 ps. In addition, MD simulations (*27*) showed that the average temperature of the protein atoms increased ~15 K after excitation of deoxyMb at 353 nm.[2] It is unlikely that such a slight temperature elevation is sufficient to influence Raman intensities. Consequently, we conclude that the observed intensity changes in the UVRR spectra mainly reflect changes in the microenvironment near the Trp and Tyr residues, such as changes in hydrogen bond strength and hydrophobicity.

Protein Structural Change near Tyrosine Residues. Horse Mb has two Tyr residues, Tyr103 and Tyr146, which are

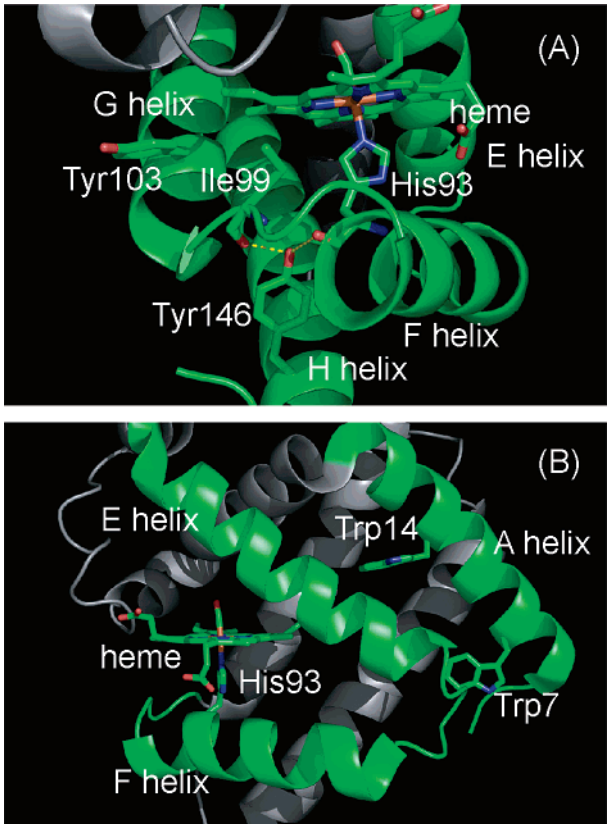

FIGURE 4: Crystallographic structure of horse Mb (*28*). (A) Close-up of the region near the two Tyr residues. (B) Close-up of the region near the two Trp residues.

involved in the G helix and in the C-terminal region of the H helix, respectively. Figure 4A depicts the crystallographic structure of horse Mb (*28*). Tyr103 is exposed to solvent in both deoxyMb and MbCO. Therefore, the Raman bands are unlikely to change in intensity upon CO photodissociation. In contrast, Tyr146 forms hydrogen bonds with the backbone carbonyl of the proximal histidine (His93) located in the F helix and with that of Ile99 located in the FG corner. The out-of-plane motion of iron following CO dissociation pushes on His93, subsequently inducing protein motion such as displacement of the F helix. Our picosecond visible resonance Raman study demonstrated that contraction of the core size concomitant with iron out-of-plane movement is completed within 2 ps (*7*, *23*). Displacement of the F helix can affect the strength of hydrogen bonding and hydrophobic interactions between Tyr146 and neighboring residues in the F helix. Therefore, a decrease in the intensity of the Y8a band at 5 ps reflects rapid F helix displacement induced by the iron out-of-plane motion.

The recovery of Y8a band intensity after the intensity decrease indicates that environmental changes near Tyr146 occur through further structural rearrangement in the F helix and/or the FG loop. The picosecond visible resonance Raman study showed that the frequency of the iron−histidine stretching mode, ν(Fe−His), exhibited a downshift at the time constant of 100 ps, suggesting the heme environment relaxes to the deoxy conformation in this time range (*7*, *23*). The transient circular dichroism (CD) signal of the N band of photodissociated MbCO showed that the orientations of aromatic chains relative to heme relaxed to the equilibrium deoxy state within 300 ps (*13*). These studies indicated structural changes in the proximal heme pocket in ~100 ps. The time scale of intensity recovery of the Y8a band was similar to that for changes in ν(Fe−His) frequency and CD signal. Since Tyr146 forms hydrogen bonds with His93 and Ile99 that compose a portion of the proximal heme pocket, the similarity of the time scale supports the interpretation that the intensity change observed in the Y8a band reflects protein motion in the vicinity of heme.

Protein Structural Changes near Tryptophan Residues. Two Trp residues are involved in horse Mb, Trp7 and Trp14, both of which are located in the A helix (Figure 4B). While Trp7 is near the protein surface, Trp14 is buried within the protein structure and contacts hydrophobic side chains of residues in the E helix. Since there is no residue that can form stable hydrogen bonds with Trp7 or Trp14, the Raman intensity changes of the Trp bands mainly reflect hydrophobicity changes in the environment near the Trp residues. An X-ray crystallographic study for sperm whale Mb showed that, from MbCO to the deoxy structure, the E and F helices rotate in a plane that contains the F helix and is perpendicular to the heme plane, keeping the relative orientations between the heme iron and the two helices unchanged (*3*). Such a movement of the EF helical sections was first proposed for Hb from nanosecond time-resolved UVRR studies by Spiro and co-workers (*19*, *29*). The direction of rotation of the E helix is toward the heme group, and therefore, this movement can change the distance between the A and E helices. Because the Trp7 and Trp14 residues are located in the interface between the A and E helices, movement of the E helix perturbs the environments of the Trp residues. Since Trp14 interacts with hydrophobic side chains in the E helix, a change in the distance between the A and E helices induces a change in environmental hydrophobicity. A Trp residue exposed to a less hydrophobic environment shifts the absorption maxima of the Trp residue to higher energies, resulting in a blue shift of the Raman excitation profile (*24*, *25*, *30*−*32*). Because the wavelength of the 226 nm probe pulse lies on the red side of the B_b absorption band, a decrease in the intensity of the Trp bands implies a decrease in local hydrophobicity. Accordingly, the decrease in intensity of the Trp bands 5 ps after CO dissociation suggests rapid movement of the E helix toward the heme group, distancing the E helix from the A helix. Rapid movement of the F helix within 5 ps also is suggested by the decrease in intensity of the Tyr Raman band. These results suggest that the primary protein response is ultrafast and involves large conformational changes, including not only displacement of the F helix but also movement of the E helix toward the heme group: the E and F helices respond to the structural change of the heme within 5 ps as if they were a single dynamical unit. Heterodyne-detected transient grating experiments demonstrated that Mb changed its overall shape within 500 fs of photolysis (*8*). The change in protein shape involved lengthening of the protein normal to the heme plane. The

[2] The actual magnitude of temperature increase would be considerably smaller than 15 K. Surrounding water was neglected in the MD simulation. With inclusion of water, energy is effectively dissipated from the protein to the water; hence, the protein experiences less heating. The simulation was conducted for photoexcited deoxyMb, which has more stored energy than photoexcited MbCO because a fraction of the absorbed energy is used for cleavage of the Fe−CO bond for MbCO.

movement of the EF helical sections significantly changes protein shape, especially normal to the direction of the heme plane; thus, these UVRR and transient grating studies provide a consistent view of the ultrafast protein motion.

In contrast to that of Mb, the movement of the EF helical sections of Hb occurs in tens of nanoseconds. The EF helical motion of Mb is more than 3 orders of magnitude faster than that of Hb (*19*, *29*). In each Hb subunit, the presence of the interhelical hydrogen bond, which is donated by the indole side chain of the Trp residue and anchors the E helix to the A helix, constrains the movement of the E helix toward the heme group. On the other hand, such an interhelical hydrogen bond does not exist in Mb. This structural difference may cause the EF helical motion to be much faster in Mb than in Hb. The alternations in the packing of the A and E helices associated with ligand binding were observed by using UVRR spectroscopy for a sol−gel encapsulated sample which slows conformational relaxation (*33*).

Intensity recovery in the nanosecond region suggests that the Trp residues are returned to a more hydrophobic environment. The UVRR study on sperm whale Mb and its Trp mutants indicated that the environment near Trp14 did not change between the deoxy and CO-bound forms, while Trp7 underwent a subtle structural change upon CO dissociation (*34*). The environment of Trp14 is affected by the degree of packing of the A and E helices. Therefore, the absence of environmental change between the deoxy and CO-bound forms suggests that the separation of the A and E helices is transient. The motion of the A helix toward the displaced E helix occurs between 1 and 2.5 ns. The time-resolved difference spectrum with the 2.5 ns time delay did not coincide with the equilibrium difference spectrum. This suggests environmental changes of Trp7 beyond 2.5 ns.

In this work, we demonstrate that picosecond time-resolved UVRR spectroscopy is a powerful technique for investigating ultrafast protein responses. Recently, time-resolved X-ray crystallography with a time resolution of 150 ps was performed to study the protein dynamics of Mb following the ligand dissociation by Anfinrud and co-workers (*35*). A combination of the two experimental techniques will provide us complementary information about ultrafast protein dynamics.

SUMMARY

Site-specific observation of picosecond protein dynamics was performed using time-resolved UVRR spectroscopy. The temporal behavior of the Trp and Tyr Raman intensity changes suggested that several phases of conformational changes in picoseconds to nanoseconds occurred upon CO dissociation. The decrease in the intensity of the Trp and Tyr Raman bands within 5 ps of dissociation indicated rapid displacement of the proximal F helix and weakened interaction between the E and A helices. These results indicate that the primary protein response is impulsively driven global motion in which the E and F helices move concertedly. Intensity recovery of Tyr bands in the sub-nanosecond region and of Trp bands in the nanosecond region suggests stepwise conformational changes occur toward the deoxy structure. We attributed these relatively slow protein motions to structural rearrangements in the proximal heme pocket followed by movement of the A helix. Elucidation of a more detailed mechanism will require determination of the contribution from each Trp or Tyr residue to the Raman intensity changes observed in transient UVRR spectra. Further investigation using Mb mutants should establish a more complete picture of the conformational relaxation of Mb.

ACKNOWLEDGMENT

We are grateful to Dr. Shoji Kaminaka for his helpful advice on the construction of the prefilter.

REFERENCES

1. Perutz, M. F., Fermi, G., Luisi, B., Shaanan, B., and Liddington, R. C. (1987) Stereochemistry of cooperative mechanisms in hemoglobin, *Acc. Chem. Res. 20*, 309−321.
2. Dickerson, R. E., and Geiss, I. (1983) *Hemoglobin: Structure, Function, Evolution, and Pathology*, Benjamin Cummings, Menlo Park, CA.
3. Kachalova, G. S., Popov, A. N., and Bartunik, H. D. (1999) A steric mechanism for inhibition of CO binding to heme proteins, *Science 284*, 473−476.
4. Petrich, J. W., Poyart, C., and Martin, J. L. (1988) Photophysics and reactivity of heme proteins: A femtosecond absorption study of hemoglobin, myoglobin, and protoheme, *Biochemistry 27*, 4049−4060.
5. Greene, B. I., Hochstrasser, R. M., Weisman, R. B., and Eaton, W. A. (1978) Spectroscopic studies of oxy- and carbonmonoxyhemoglobin after pulsed optical excitation, *Proc. Natl. Acad. Sci. U.S.A. 75*, 5255−5259.
6. Srajer, V., Ren, Z., Teng, T. Y., Schmidt, M., Ursby, T., Bourgeois, D., Pradervand, C., Schildkamp, W., Wulff, M., and Moffat, K. (2001) Protein conformational relaxation and ligand migration in myoglobin: A nanosecond to millisecond molecular movie from time-resolved Laue X-ray diffraction, *Biochemistry 40*, 13802−13815.
7. Mizutani, Y., and Kitagawa, T. (2001) Ultrafast structural relaxation of myoglobin following photodissociation of carbon monoxide probed by time-resolved resonance Raman spectroscopy, *J. Phys. Chem. B 105*, 10992−10999.
8. Goodno, G. D., and Miller, R. J. D. (1999) Femtosecond heterodyne-detected four-wave-mixing studies of deterministic protein motions. II. Theory and experimental technique of diffractive optics-based spectroscopy, *J. Phys. Chem. A 103*, 10619−10629.
9. Causgrove, T. P., and Dyer, R. B. (1996) Picosecond structural dynamics of myoglobin following photolysis of carbon monoxide, *J. Phys. Chem. 100*, 3273−3277.
10. Lim, M., Jackson, T. A., and Anfinrud, P. A. (1997) Ultrafast rotation and trapping of carbon monoxide dissociated from myoglobin, *Nat. Struct. Biol. 4*, 209−214.
11. Lim, M., Jackson, T. A., and Anfinrud, P. A. (1995) Binding of CO to myoglobin from a heme pocket docking site to form nearly linear Fe−C−O, *Science 269*, 962−966.
12. Lim, M., Jackson, T. A., and Anfinrud, P. A. (1993) Nonexponential protein relaxation: Dynamics of conformational change in myoglobin, *Proc. Natl. Acad. Sci. U.S.A. 90*, 5801−5804.
13. Xie, X. L., and Simon, J. D. (1991) Protein conformational relaxation following photodissociation of CO from carbonmonoxymyoglobin: Picosecond circular dichroism and absorption studies, *Biochemistry 30*, 3682−3692.
14. Ansari, A., Jones, C. M., Henry, E. R., Hofrichter, J., and Eaton, W. A. (1992) The role of solvent viscosity in the dynamics of protein conformational changes, *Science 256*, 1796−1798.
15. Jackson, T. A., Lim, M., and Anfinrud, P. A. (1994) Complex nonexponential relaxation in myoglobin after photodissociation of MbCO: Measurement and analysis from 2 ps to 56 μs, *Chem. Phys. 180*, 131−140.
16. Kitagawa, T. (1992) Investigation of higher order structures of proteins by ultraviolet resonance Raman spectroscopy, *Prog. Biophys. Mol. Biol. 58*, 1−18.
17. Harada, I., and Takeuchi, H. (1986) in *Advances in Spectroscopy: Spectroscopy of Biological Systems* (Clark, R. J. H., and Hester, R. E., Eds.) pp 113−175, Wiley, New York.
18. Asher, S. A., Bormett, R. W., Chen, X. G., Lemmon, D. H., Cho, N., Peterson, P., Arrigoni, M., Spinelli, L., and Cannon, J. (1993) UV Resonance Raman Spectroscopy Using a New cw Laser

Source: Convenience and Experimental Simplicity, *Appl. Spectrosc. 47*, 628−633.
19. Jayaraman, V., Rodgers, K. R., Mukerji, I., and Spiro, T. G. (1995) Hemoglobin allostery: Resonance Raman spectroscopy of kinetic intermediates, *Science 269*, 1843−1848.
20. Hashimoto, S., Sasaki, M., Takeuchi, H., Needleman, R., and Lanyi, J. K. (2002) Changes in hydrogen bonding and environment of tryptophan residues on helix F of bacteriorhodopsin during the photocycle: A time-resolved ultraviolet resonance Raman study, *Biochemistry 41*, 6495−6503.
21. Kim, J. E., Pan, D., and Mathies, R. A. (2003) Picosecond dynamics of G-protein coupled receptor activation in rhodopsin from time-resolved UV resonance Raman spectroscopy, *Biochemistry 42*, 5169−5175.
22. Kaminaka, S., and Mathies, R. A. (1998) High-throughput large-aperture prism prefilter for ultraviolet resonance Raman spectroscopy, *Appl. Spectrosc. 52*, 469−473.
23. Mizutani, Y., and Kitagawa, T. (2001) Ultrafast dynamics of myoglobin probed by time-resolved resonance Raman spectroscopy, *Chem. Rec. 1*, 258−275.
24. Chi, Z., and Asher, S. A. (1998) UV Raman determination of the environment and solvent exposure of Tyr and Trp residues, *J. Phys. Chem. B 102*, 9595−9602.
25. Matsuno, M., and Takeuchi, H. (1998) Effects of hydrogen bonding and hydrophobic interactions on the ultraviolet resonance Raman intensities of indole ring vibrations, *Bull. Chem. Soc. Jpn. 71*, 851−857.
26. Lian, T., Locke, B., Kholodenko, Y., and Hochstrasser, R. M. (1994) Energy Flow from Solute to Solvent Probed by Femtosecond IR Spectroscopy: Malachite Green and Heme Protein Solutions, *J. Phys. Chem. 98*, 11648−11656.
27. Henry, E. R., Eaton, W. A., and Hochstrasser, R. M. (1986) Molecular dynamics simulations of cooling in laser-excited heme proteins, *Proc. Natl. Acad. Sci. U.S.A. 83*, 8982−8986.
28. Chu, K., Vojtechovsky, J., McMahon, B. H., Sweet, R. M., Berendzen, J., and Schlichting, I. (2000) Structure of a New Ligand Binding Intermediate in Wild-type Carbonmonoxy Myoglobin, *Nature 403*, 921−923.
29. Rodgers, K. R., and Spiro, T. G. (1994) Nanosecond dynamics of the RT transition in hemoglobin: Ultraviolet Raman studies, *Science 265*, 1697−1699.
30. Takeuchi, H. (2003) Raman structural markers of tryptophan and histidine side chains in proteins, *Biopolymers 72*, 305−317.
31. Takeuchi, H., Ohtsuka, Y., and Harada, I. (1992) Ultraviolet resonance Raman study on the binding mode of enkephalin to phospholipid membranes, *J. Am. Chem. Soc. 114*, 5321−5328.
32. Efremov, R. G., Feofanov, A. V., and Nabiev, I. R. (1992) Effect of hydrophobic environment on the resonance Raman spectra of tryptophan residues in proteins, *J. Raman Spectrosc. 23*, 69−73.
33. Juszczak, L. J., and Friedman, J. M. (1999) UV Resonance Raman Spectra of Ligand Binding Intermediates of Sol−Gel Encapsulated Hemoglobin, *J. Biol. Chem. 274*, 30357−30360.
34. Haruta, N., Aki, M., Ozaki, S., Watanabe, Y., and Kitagawa, T. (2001) Protein conformation change of myoglobin upon ligand binding probed by ultraviolet resonance Raman spectroscopy, *Biochemistry 40*, 6956−6963.
35. Hummer, G., Schotte, F., and Anfinrud, P. A. (2004) Unveiling functional protein motions with picosecond X-ray crystallography and molecular dynamics simulations, *Proc. Natl. Acad. Sci. U.S.A. 101*, 15330−15334.

BI051732C